

Statistical analysis of light fragment production from medium energy proton-induced reactions

S. Furihata*

TRIUMF, Vancouver, British Columbia, Canada V6T 2A3

Mitsubishi Research Institute Inc., 2-3-6 Otemachi, Chiyoda-ku, Tokyo 100-8141, Japan

(April 26, 2024)

Abstract

The light fragment production reactions for 10 MeV to 3 GeV protons incident on ^{16}O , ^{27}Al , $^{\text{nat}}\text{Fe}$, ^{93}Nb , and $^{\text{nat}}\text{Ag}$ are analyzed by a combination of an intranuclear cascade model and a generalized evaporation model which includes light nuclei up to Mg as ejectiles. It is concluded that evaporation is the dominant process by which particles lighter than or equal to Be are produced from targets heavier than O.

Typeset using REVTEX

*Fax : +1-604-222-1074, email: furihata@triumf.ca

I. INTRODUCTION

Fragment and residual nuclei production has attracted many people's interests, not only nuclear physicists but also astrophysicists and nuclear engineers. The production of intermediate mass fragments from high energy proton-nucleus reactions or nucleus-nucleus reactions has been a hot topic in nuclear physics for a decade [1,2]. Astrophysics and cosmic ray physics have been interested in residual nuclei production in order to calculate the production of cosmogenic nuclides in extraterrestrial matter by solar and galactic cosmic rays. Recently, nuclear engineering has needed the particle production cross sections for the development of accelerator-based systems for transmutation of radioactive nuclear waste. From the radiation safety aspect, it has also become more important to estimate the amount of radioactivity produced from various targets, as new applications of high energy proton accelerators, such as spallation neutron sources and the production of beams of unstable nuclei are being developed.

In 1997, the Organization for Economic Cooperation and Development (OECD) Nuclear Energy Agency (NEA) conducted benchmark calculations on activation yields to determine the predictive power of current nuclear reaction models and codes [3]. The results calculated using many different codes which are based on a combination of different models, such as the intranuclear cascade model (INC), the exciton model, the evaporation-fission model, the quantum molecular dynamics model and the statistical multifragmentation model, were compared with experimental data. It became clear that most of the computer codes did not reproduce light fragment production reactions, such as $\text{Fe}(p,X)^7\text{Be}$, especially at low proton-incident energy. They considered that an adequate description of the Fermi break-up model [4] and a fragmentation model was urgently needed.

The evaporation model has been very successful in describing residual nuclei production from hot nuclei. In many codes, not only those codes that were used in the benchmark calculation by OECD/NEA, but also the codes that are widely used for shielding calculations, such as the LAHET code [5], the evaporation model is used to describe the de-excitation of thermalized nuclei. Despite its success, the model has not been used to describe light fragment emission, except for a few studies concerning break-up of highly excited nuclei [1,6].

In this study, we propose a generalized evaporation model (GEVAP) for Monte Carlo simulation, based on the Weisskopf-Ewing model [7,8]. Nucleons and helium nuclei are the dominant particles emitted from an excited nucleus. Therefore, only these particles are treated as ejectiles in the Dostrovsky's evaporation models [9] implemented in the LAHET code [5]. On the other hand, some studies [1,6] consider light nuclei heavier than α particles as ejectiles since there is no reason that those particles can not be emitted from excited nuclei via evaporation process. In our generalized evaporation model, 66 nuclides up to Mg are included as ejectiles, not only in their ground states but also in their excited states. Besides, we use the accurate level density function for the total decay width calculation instead of an approximate form of level density function which is used in the Dostrovsky's evaporation models [9].

Light fragments produced from proton-induced reactions are analyzed by the combination of the INC model implemented in the LAHET code [5] and the generalized evaporation model (GEVAP). In order to estimate light particle production from a nucleon-nucleus re-

action by the generalized evaporation model, we have to assume the ensemble of hot nuclei which are produced after the initial non-equilibrium stage. Since the excitation energy, the mass, and the charge of the hot residual nuclei produced from high energy reaction are widely distributed, we can not use the simple assumption that a single excited nucleus represents the ensemble of hot thermalized nuclei. However, the INC model can provide an ensemble of residual nuclei with broad distribution in excitation energy, nuclear mass and charge. The LAHET code employs the Bertini intranuclear cascade model [10] for a non-equilibrium stage of nuclear reaction, and the Fermi break-up model [4] and the evaporation model proposed by Dostrovsky *et al.* [9] for a thermalized stage. Mass A_i , charge Z_i , excitation energy E , recoil energy, and the direction of recoil motion are extracted from the INC calculation done by the LAHET code. Then the de-excitation process of the hot nucleus with these quantities are calculated by GEVAP, instead of by the Fermi break-up model and the evaporation model employed in the LAHET code. In the following, we call this calculation procedure ‘INC/GEVAP’.

We focus mainly on ^7Be produced by proton-induced reactions in the energy range from 10 MeV to 3 GeV, because ^7Be is the most intensively measured light fragment produced from various targets, and many experimental data are available for comparison. We compare the INC/GEVAP results with experimental data as well as the results calculated by using LAHET, to make the effect of using different de-excitation models clear.

II. THE GENERALIZED EVAPORATION MODEL

Let us consider that a parent nucleus i with an excited energy $E[\text{MeV}]$, a mass number A_i , and a charge number Z_i emits a particle j in its ground state with A_j and Z_j , and becomes a daughter nucleus d with A_d and Z_d . According to the Weisskopf’s formulation [7], the decay probability P_j with total kinetic energy in the center-of-mass system between ϵ and $\epsilon + d\epsilon$ is expressed as

$$P_j(\epsilon)d\epsilon = g_j \sigma_{inv}(\epsilon) \frac{\rho_d(E - Q - \epsilon)}{\rho_i(E)} \epsilon d\epsilon, \quad (1)$$

where σ_{inv} is the cross section for the inverse reaction, ρ_i and ρ_d are level densities [MeV^{-1}] of the parent and the daughter nucleus, respectively. With the spin S_j and the mass m_j of the emitted particle j , g_j is expressed as $g_j = (2S_j + 1)m_j/\pi^2\hbar^2$. In this study we use the Audi-Wapstra mass table [11] to calculate the Q-values Q for emission of particle j .

The cross section for the inverse reaction σ_{inv} is expressed as [9]

$$\sigma_{inv}(\epsilon) = \begin{cases} \sigma_g c_n (1 + b/\epsilon) & \text{for neutrons} \\ \sigma_g c_j (1 - V/\epsilon) & \text{for charged particles} \end{cases} \equiv \sigma_g \alpha \left(1 + \frac{\beta}{\epsilon}\right), \quad (2)$$

where $\sigma_g = \pi R_b^2$ [fm^2] is the geometric cross section, and $V = Z_j Z_d e^2 / R_c$ is the Coulomb barrier.

In this study, we use the parameter set determined by Dostrovsky *et al.* [9] and Matsuse *et al* [12]. Dostrovsky *et al.* [9] determined c_n , c_j , b , R_b , and R_c for n, p, d, t, ^3He , and α emission by fitting the expression to the theoretical calculation done by Shapiro [13] and Blatt and

Weisskopf [14], so that the effect of overlapping wave functions was taken into account. These parameters are used in the Dostrovsky's evaporation model [9] implemented in LAHET [5]. Meanwhile, Matsuse *et al.* determined the critical distance (R_b and R_c , with $c_j = 1$) by fitting Eq. (2) to experimental fusion cross sections for heavy ion reactions. We use the Dostrovsky's parameters for n, p, d, t, ${}^3\text{He}$, and α emission and the Matsuse's parameters for other particles. In the following we call these parameters "the precise parameter set". Besides the calculation with the precise parameter set, we use the simple parameter set, given by $c_n = c_j = 1$, $b = 0$ and $R_b = R_c = r_0(A_j^{1/3} + A_d^{1/3})$ [fm] for the inverse cross section. In the calculation with the simple parameter set, values of $r_0 = 1.2$, 1.5, and 2.0 are tried to test the stability of our model.

The total decay width Γ_j can be calculated by integrating Eq. (1) with respect to the total kinetic energy ϵ from the Coulomb barrier V up to the maximum possible value ($E - Q$). By using Eq. (2) for σ_{inv} , the total decay width for the particle emission is expressed as

$$\Gamma_j = \frac{g_j \sigma_g \alpha}{\rho_i(E)} \int_V^{E-Q} \epsilon \left(1 + \frac{\beta}{\epsilon}\right) \rho_d(E - Q - \epsilon) d\epsilon. \quad (3)$$

According to the Fermi-gas model, the total level density $\rho(E)$ of a nucleus summed over all the possible states with the angular momenta is given by the expression [15]

$$\rho(E) = \frac{\pi}{12} \frac{e^{2\sqrt{a(E-\delta)}}}{a^{1/4}(E-\delta)^{5/4}} \quad \text{for } E \geq E_x, \quad (4)$$

where $a = A_d/8$ [MeV $^{-1}$] is the level density parameter, and δ [MeV] is the pairing energy of the daughter nucleus evaluated by Cook *et al.* [16]. For those values not evaluated by Cook *et al.*, δ obtained by Gilbert and Cameron [15] are used. E_x is determined by Gilbert and Cameron [15] as $E_x = U_x + \delta$ where $U_x = 2.5 + 150/A_d$. In the calculation with the precise parameter set, we use the Gilbert-Cameron-Cook-Ignatyuk (GCCI) level density parameter [5], in which the pairing corrections and the energy dependence of the level density parameter are taken into account, instead of the simple expression $a = A_d/8$. The GCCI level density parameter is employed in the LAHET code [5].

When E is below E_x , instead of Eq. (4) the following formula gives a good fit to the experimental level densities [15]:

$$\rho(E) = \frac{1}{T} e^{(E-E_0)/T} \quad \text{for } E < E_x, \quad (5)$$

where T is the nuclear temperature given by $1/T = \sqrt{a/U_x} - 1.5/U_x$. To connect Eq. (4) and Eq. (5) smoothly, E_0 is defined as $E_0 = E_x - T(\log T - 0.25 \log a - 1.25 \log U_x + 2\sqrt{aU_x})$.

We use the expressions Eq. (4) and Eq. (5) to calculate the total decay width. The simple form $\rho \propto \exp(2\sqrt{a(E-\delta)})$, which is used in the Dostrovsky's evaporation models [9], is a good approximation when the residual excitation energy is high, however, it is not applicable for residual nuclei with small mass and low excitation energy.

When $E - Q - V$ is below E_x , Eq. (3) can be solved analytically, by substituting Eq. (5) into Eq. (3).

$$\Gamma_j = \frac{\pi g_j \sigma_g \alpha}{12 \rho_i(E)} \{I_1(t, t) + (\beta + V) I_0(t)\} \text{ for } E - Q - V < E_x, \quad (6)$$

where $I_0(t)$ and $I_1(t, t_x)$ are expressed as:

$$I_0(t) = e^{-E_0/T} (e^t - 1),$$

$$I_1(t, t_x) = e^{-E_0/T} T \{(t - t_x + 1) e^{t_x} - t - 1\},$$

where $t = (E - Q - V)/T$ and $t_x = E_x/T$. When $E - Q - V$ is greater than E_x , the integral of Eq. (3) can not be solved analytically because of the denominator in Eq. (4). However, it is expressed approximately as

$$\Gamma_j = \frac{\pi g_j \sigma_g \alpha}{12 \rho_i(E)} [I_1(t, t_x) + I_3(s, s_x) e^s + (\beta + V) \{I_0(t_x) + I_2(s, s_x) e^s\}] \text{ for } E - Q - V \geq E_x. \quad (7)$$

where $I_2(s, s_x)$ and $I_3(s, s_x)$ are given by:

$$I_2(s, s_x) = 2\sqrt{2} \left\{ s^{-3/2} + 1.5s^{-5/2} + 3.75s^{-7/2} - (s_x^{-3/2} + 1.5s_x^{-5/2} + 3.75s_x^{-7/2}) e^{s_x - s} \right\},$$

$$I_3(s, s_x) = (\sqrt{2}a)^{-1} \left[2s^{-1/2} + 4s^{-3/2} + 13.5s^{-5/2} + 60.0s^{-7/2} + 325.125s^{-9/2} - \left\{ (s^2 - s_x^2) s_x^{-3/2} \right. \right.$$

$$+ (1.5s^2 + 0.5s_x^2) s_x^{-5/2} + (3.75s^2 + 0.25s_x^2) s_x^{-7/2} + (12.875s^2 + 0.625s_x^2) s_x^{-9/2}$$

$$\left. \left. + (59.0625s^2 + 0.9375s_x^2) s_x^{-11/2} + (324.8s^2 + 3.28s_x^2) s_x^{-13/2} \right\} e^{s_x - s} \right],$$

with $s = 2\sqrt{a(E - Q - V - \delta)}$ and $s_x = 2\sqrt{a(E_x - \delta)}$.

In the present Monte Carlo simulation, ejectile j is selected according to the probability distribution calculated as $p_j = \Gamma_j / \sum_j \Gamma_j$, where Γ_j is given by Eqs. (6) or (7). The total kinetic energy ϵ of the emitted particle j and the daughter nucleus is chosen according to the probability distribution given by Eq. (1). The angular distribution of the motion is randomly selected to be isotropic in the center-of-mass system. The excitation energy of the daughter nucleus E_d is calculated as $E_d = E - Q - \epsilon$.

In this study, we consider 66 nuclides as ejectiles, not only in their ground states but also in their excited states. It is important to include excited states in the particles emitted via the evaporation process, because it greatly enhances the yield of heavy particle emission [6]. The selected ejectiles satisfy the following criteria: (1) isotopes with $Z_j \leq 12$; (2) naturally existing isotopes or isotopes near the stability line; (3) isotopes with half-life longer than 1 ms. The selected ejectiles are listed in Table I.

If the mean lifetime of a resonance is longer than the decay width of the resonance emission, such a resonance can survive during the evaporation process. The excited state is included if its half lifetime $T_{1/2}$ [sec] satisfies the following condition:

$$\frac{T_{1/2}}{\ln 2} > \frac{\hbar}{\Gamma_j^*}, \quad (8)$$

where Γ_j^* is the decay width of the resonance emission. Γ_j^* can be calculated in the same manner as for a ground state particle emission. The Q-value for the resonance emission is

expressed as $Q^* = Q + E_j^*$, where E_j^* is the excitation energy of the resonance. The spin state of the resonance S_j^* is used in the calculation of g_j , instead of the spin of the ground state S_j . We use the ground state mass m_j for excited states because the difference between the masses is negligible.

Instead of treating a resonance as an independent particle, we simply enhance the decay width of the ground state particle emission. We redefine the decay width Γ_j as

$$\Gamma_j = \Gamma_j^0 + \sum_n \Gamma_j^n, \quad (9)$$

where Γ_j^0 is the decay width of the ground state particle j emission, and Γ_j^n is that of the n th excited state of the particle j emission which satisfies Eq. (8).

The total kinetic energy distribution of the excited particle emission is assumed to be the same as that of the ground state particle emission. S_j^* , E_j^* , and $T_{1/2}$ used in this study are extracted from the Evaluated Nuclear Structure Data File (ENSDF) database maintained by the National Nuclear Data Center [17].

III. COMPARISON WITH EXPERIMENTAL DATA

The excitation functions of ${}^7\text{Be}$ produced by proton reactions on ${}^{16}\text{O}$, ${}^{27}\text{Al}$, ${}^{\text{nat}}\text{Fe}$, and ${}^{93}\text{Nb}$ are shown in Fig. 1. The results calculated by INC/GEVAP with the precise parameter set, which consists of the parameters for inverse reactions determined by Dostrovsky *et al.* [9] and Matsuse *et al* [12] and the GCCI level density parameter, are shown by the solid lines. The estimates by INC/GEVAP with $r_0 = 1.5$ and those by LAHET are also shown in the figures as well as the experimental data collected in Ref. [3]. The results by INC/GEVAP with $r_0 = 1.2$ and 2.0 are represented only for the Nb target, because there is less difference in the results for other targets. For the O target, the differences in the estimates between by INC/GEVAP with $r_0 = 1.5$ and by that with $r_0 = 1.2$ or 1.5 are 20 %, except at the threshold energy. For Al target, the differences are within a factor of two in the whole energy region. INC/GEVAP with $r_0 = 2.0$ produces almost the same cross sections for the $\text{Fe}(\text{p},\text{X}){}^7\text{Be}$ reaction as those with precise parameter set, and the differences are within 20 %. In the whole energy region, for all the targets, INC/GEVAP produces more ${}^7\text{Be}$ as r_0 increases. The estimates by INC/GEVAP for Al with $r_0 = 1.5$ give the best agreement with the experimental data, as seen the dashed line lying underneath the measurement points in the whole energy region in Fig. 1 (b). Whereas for Fe and Nb INC/GEVAP with the precise parameter set reproduce the excitation functions better than that with the simple parameter set, and the estimates agree with most of the experimental data within 50 %.

INC/GEVAP reproduces the excitation functions for all the targets, whereas LAHET fails to reproduce the shape of the excitation functions except for the O target. The shapes of the excitation functions estimated by INC/GEVAP do not change with the choice of the parameter sets. Since LAHET severely underestimates the ${}^7\text{Be}$ productions from Al below 300 MeV, Fe and Nb below 3 GeV, it is obvious that the Fermi break-up is not the dominant process for the ${}^7\text{Be}$ productions in these reactions.

The isotopic distributions of H, He, Li, and Be nuclei produced from 2100 MeV proton incident on ${}^{16}\text{O}$ and from 480 MeV proton incident on ${}^{\text{nat}}\text{Ag}$ are shown in Fig 2. The results

estimated by INC/GEVAP with the precise parameter set (the open squares) are shown as well as the experimental data for the O target measured by Olsen *et al.* [18], and the data for the Ag target by Green *et al.* [19] (the closed circles). INC/GEVAP reproduces the isotopic distributions for both these reactions, and the estimates agree with most of the measurements with 50 % accuracy.

IV. SUMMARY AND CONCLUSION

We have formulated a generalized evaporation model (GEVAP) based on the Weisskopf-Ewing model [7,8]. The features of the model are: (1) the accurate level density function is used for deriving the decay width of particle emission; (2) sixty-six nuclides up to Mg, not only in their ground state but also in their excited states, are taken into account in this study.

The combination of the intranuclear cascade model (INC) and GEVAP successfully reproduces the excitation functions of ^7Be produced by protons incident on ^{16}O , ^{27}Al , $^{\text{nat}}\text{Fe}$, and ^{93}Nb . The choice of the parameter set in GEVAP does not affect the resulting shapes of the excitation functions. INC/GEVAP also predicts the isotopic distributions of H, He, Li, and Be produced from O and Ag with 50 % accuracy.

From the results, it is concluded that the evaporation process is the main process via which particles lighter than or equal to Be are produced by protons incident on targets heavier than O. INC/GEVAP can predict the production cross sections of particles lighter or equal to Be between 50 % to a factor of two in accuracy depending on the choice of the parameter set used in GEVAP. In this study, the precise parameter set gives the best results for overall reactions, and the accuracy is 50 % on the average.

ACKNOWLEDGMENTS

The author would like to thank Dr. T. Numao for useful discussion and encouragements, and also Dr. L. Moritz, Dr. G. Greeniaus, Dr. P. Jackson and Dr. R. Korteling for valuable comments on this paper, and Dr. R. E. Prael for supplying the LAHET code. The author also appreciates the TRIUMF computer group for providing a computer for the calculations.

REFERENCES

- [1] J. P. Bondorf, A. S. Botvina, A. S. Iljinov, I. N. Mishustin, and K. Sneppen, Phys. Rep. **257**, 133 (1995).
- [2] J. Hufner, Phys. Rep. **125**, 129 (1985).
- [3] R. Michel and P. Nagel, *International Codes and Model Intercomparison for Intermediate Energy Activation Yields*, OECD/NEA, NSC/DOC(97)-1, 1997.
- [4] E. Fermi, Prog. Theo. Phys. **5**, 570 (1950).
- [5] R. E. Prael and H. Lichtenstein, *User Guide to LCS: The LAHET Code System*, Los Alamos National Laboratory, LA-UR-89-3014, 1989.
- [6] W. A. Friedman and W. G. Lynch, Phys. Rev. C **28**, 16 (1983).
- [7] V. F. Weisskopf, Phys. Rev. **52**, 295 (1937).
- [8] V. F. Weisskopf and P. H. Ewing, Phys. Rev. **57**, 472 (1940).
- [9] I. Dostrovsky, Z. Fraenkel, and G. Friedlander, Phys. Rev. **116**, 683 (1959).
- [10] H. W. Bertini, Phys. Rev. **188**, 1711 (1969).
- [11] G. Audi and A. H. Wapstra, Nucl. Phys. **A595**, 409 (1995).
- [12] T. Matsuse, A. Arima, and S. M. Lee, Phys. Rev. C **26**, 2338 (1982).
- [13] M. M. Shapiro, Phys. Rev. **90**, 171 (1953).
- [14] J. Blatt and F. Weisskopf, *Theoretical Nuclear Physics* (John Wiley & Sons, Inc., New York, USA, 1952), p. 345.
- [15] A. Gilbert and A. G. W. Cameron, Can. J. Phys. **43**, 1446 (1965).
- [16] J. L. Cook, H. Ferguson, and A. R. D. Musgrove, Aust. J. Phys. **20**, 477 (1967).
- [17] The Evaluated Structure Data File (ENDSF) maintained by the National Nuclear Data Center (NNDC), Brookhaven National Laboratory, <http://www.nndc.bnl.gov/>.
- [18] D. L. Olson, B. L. Berman, D. E. Greiner, H. H. Heckman, P. J. Lindstrom, and H. J. Crawford, Phys. Rev. C **28**, 1602 (1983).
- [19] R. E. L. Green, R. G. Korteling, and K. P. Jackson, Phys. Rev. C **29**, 1806 (1984).
- [20] R. Michel *et al.*, Nucl. Inst. Meth. in Phys. Res. B **129**, 153 (1997), data retrieved from the NNDC (EXFOR 00276).
- [21] B. Dittrich, U. Herpers, M. Lupke, R. Michel, H. J. Hofmann, and W. Wolfli, Radiochim. Acta **50**, 11 (1990), data retrieved from the NNDC (EXFOR 00098).

FIGURES

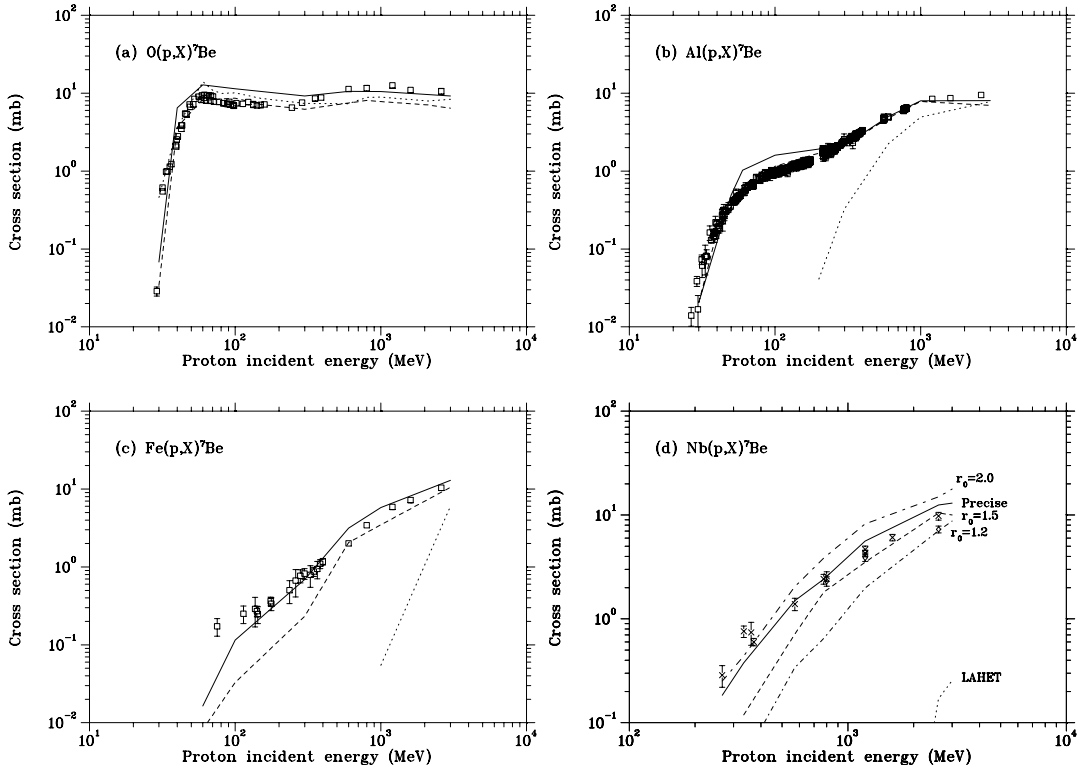


FIG. 1. The excitation function of ${}^7\text{Be}$ produced from ${}^{16}\text{O}$, ${}^{27}\text{Al}$, ${}^{\text{nat}}\text{Fe}$ and ${}^{93}\text{Nb}$: The estimates by INC/GEVAP with $r_0 = 1.5$ and the precise parameter set are shown by the dashed lines and the solid lines. The results calculated by using LAHET are shown by the dotted lines. The open squares are the experimental data collected in Ref. [3], and the crosses and the open diamonds are experimental data in Ref. [20] and Ref. [21], respectively.

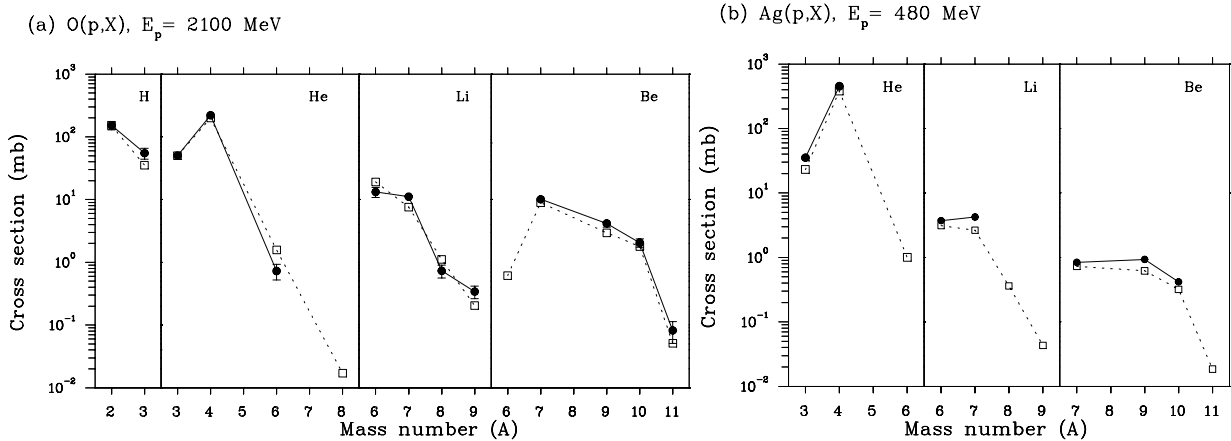


FIG. 2. The isotopic distributions of the nuclei produced from: (a) 2100 MeV protons incident on ${}^{16}\text{O}$; (b) 480 MeV protons incident on ${}^{\text{nat}}\text{Ag}$. The open squares with the solid lines denotes the results by calculated INC/GEVAP with the precise parameter set, and the black circles with the dashed lines denotes experimental data [18,19]. The lines are drawn to guide to eyes.

TABLES

TABLE I. The ejectiles considered in this study

Z_j	Ejectiles						
0	n						
1	p	d	t				
2	^3He	^4He	^6He	^8He			
3	^6Li	^7Li	^8Li	^9Li			
4	^7Be	^9Be	^{10}Be	^{11}Be	^{12}Be		
5	^8B	^{10}B	^{11}B	^{12}B	^{13}B		
6	^{10}C	^{11}C	^{12}C	^{13}C	^{14}C	^{15}C	^{16}C
7	^{12}N	^{13}N	^{14}N	^{15}N	^{16}N	^{17}N	
8	^{14}O	^{15}O	^{16}O	^{17}O	^{18}O	^{19}O	^{20}O
9	^{17}F	^{18}F	^{19}F	^{20}F	^{21}F		
10	^{18}Ne	^{19}Ne	^{20}Ne	^{21}Ne	^{22}Ne	^{13}Ne	^{24}Ne
11	^{21}Na	^{22}Na	^{23}Na	^{24}Na	^{25}Na		
12	^{22}Mg	^{23}Mg	^{24}Mg	^{25}Mg	^{26}Mg	^{27}Mg	^{28}Mg